Iranian Food Science and Technology Research Journal
Vol. 19, No. 3, Aug.-Sep. 2023, p. 15-31

نشریه پژوهشهای علوم و صنایع غذایی ایران
جلد ۱۹، شماره ۳، مرداد- شهریور ۱۴۰۲ ص. ۳۱-۱۵



Research Article
Homepage: http://ifstrj.um.ac.ir

# Encapsulation of Coenzyme $Q_{10}$ by Gelatin–basil Seed Mucilage Using Complex Coacervation: Optimization, Physicochemical Characterizations and Milk Fortification

**S. Ramezani[1], M. Shahedi[2], M. Fathi[3]***

Received: 2023.03.17
Revised: 2023.06.14
Accepted: 2023.06.28
Available Online: 2023.06.28

**How to cite this article:**
Ramezani, S., Shahedi, M., & Fathi, M. (2023). Encapsulation of coenzyme $Q_{10}$ by gelatin–basil seed mucilage using complex coacervation: Optimization, physicochemical characterizations and milk fortification. *Iranian Food Science and Technology Research Journal, 19*(3), 15-31. https://doi.org/10.22067/ifstrj.2023.81438.1240

## Abstract

Global concern about human health and the increase the prevalence of chronic diseases in recent years lead to growing appeals for nutritious and healthy compounds, such as coenzyme $Q_{10}$. Susceptibility to heat and lipophilic properties of coenzyme $Q_{10}$ limit its utilization in food. Encapsulation is a technology that protects bioactive ingredients from harsh environmental conditions and extends shelf life. The purpose of this study was to encapsulate coenzyme $Q_{10}$ using complex coacervation by gelatin–basil seed mucilage and characterize physical, thermal and chemical properties of produced microcapsules. Response surface methodology was applied to determine the optimum level of the four formulation variables for maximum encapsulation efficiency, loading capacity and turbidity and minimum supernatant absorption. The optimum microcapsules had encapsulation efficiency of 83.69%, encapsulation load of 16.32%, turbidity of 0.979 and supernatant absorption of 0.227. The microcapsules were assessed by scanning electron microscopy, Fourier transform infrared spectroscopy, and differential scanning calorimetry. The results of FTIR confirmed the formation of coacervates. The thermogram of $Q_{10}$ loaded microcapsule melting point was not observed at its melting point (50°C) due to its solubility in the oil phase and appropriate entrapment. Release behavior of $Q_{10}$ was studied by different mathematical models. Microencapsulated $Q_{10}$ was used to fortify milk and the results showed that the developed protein-carbohydrate microcapsules can be applied for protection of hydrophobic compounds.

**Keywords:** Basil seed mucilage, Coenzyme $Q_{10}$, Encapsulation, Gelatin, Physicochemical characterizations

## Introduction

Coenzyme $Q_{10}$ was first discovered by Professor Fredricke L. Crane in 1957. It is a natural and efficient antioxidant that is found in the human body in both of reduction and oxidation form (Wang *et al.*, 2023). The $Q_{10}$ is one of the main parts of electron transport chain in the mitochondria. It has an essential function in metabolism of mitochondrial energy and is responsible for converting energy from carbohydrate, protein, fatty acid to adenosine triphosphate (ATP). The $Q_{10}$ is a reinforcer of immune function and it is an improver of muscular dystrophy, exercise capacity, heart function and overall quality of life (Li *et al.*, 2023).

Microencapsulation is a technology that protects various food ingredients from the environment and controls their release to target specific sites or meliorates their flow and

1, 2 and 3- M.Sc. Student, Professor and Associate Professor, Department of Food Science and Technology, College of Agriculture, Isfahan University of Technology, Isfahan, Iran, respectively.

(*- Corresponding Author Email: mfathi@iut.ac.ir)
DOI: 10.22067/ifstrj.2023.81438.1240

organoleptic properties. Various methods for preparation of microcapsules have been widely introduced, such as the phase separation, extrusion method, complex coacervation and polycondensation. Among these, complex coacervation is considered an excellent method for microencapsulation because of the simple experiment process and high loading capacity. Complex coacervation is used in food industry for encapsulation of bioactive ingredients. When two or more oppositely charged polyelectrolytes are combined under a reasonable condition, two phases are created, including polymer rich phase and polymer poor phase. The former phase is a dense soluble that participates in the process of encapsulating (Yang *et al.*, 2015). Many studies have been reported on complex coacervation of proteins and polysaccharides, such as gelatin/gum Arabic (Dong *et al.*, 2011), soybean protein isolate/pectin (Hu *et al.*, 2023), whey protein/gum Arabic (Sharifi *et al.*, 2021), canola protein isolate/chitosan (Chang *et al.*, 2016), gelatin/acacia gum (Nakagawa and Nagao, 2012) and gelatin/pectin (Byeon *et al.*, 2023).

Basil seed is obtained from the basil plant (*Ocimum basilicum*), which belongs to the Labiatae family. It has high mucilaginous components, which is classified as anion hydrocolloids. The mucilage of basil seed has been used in the food industry as a functional ingredient because of its potential applications as a thickening and stabilizing properties (Hosseini-Parvar *et al.*, 2010; Razavi *et al.*, 2010).

To the best of our knowledge, there is no work on complex coacervation involving basil seed mucilage and gelatin. Basil seed mucilage and gelatin are appropriate to be used to form coacervates as gelatin is positively charged below its isoelectric point, while basil seed mucilage is negatively charged in a wide pH range. Therefore the aims of this research were to encapsulate coenzyme $Q_{10}$ by complex coacervation using basil seed mucilage and gelatin and characterize physicochemical properties of produced microcapsules. Effects of the gelatin percentage, basil seed mucilage percentage, oil phase percentage, and pH on the encapsulation efficiency (EE), encapsulation load (EL), turbidity, and supernatant absorbance were also assessed. Scanning electron microscopy, Fourier transform infrared (FTIR) spectroscopy, and differential scanning calorimetry (DSC) were used to characterize microcapsule properties.

## Materials and Methods

### Materials

Bovine gelatin was obtained from Global Capsule Company (Bangladesh). Basil seed was purchased from a local market (Esfahan, Iran). Coenzyme $Q_{10}$ was obtained from Zhejiang Nhu Company (China). Sunflower oil was provided from Varamin Company (Iran). N-hexane was obtained from Sepahan Company (Iran). Methanol and n-hexane were HPLC grade and obtained from Merck Company (Germany).

### Mucilage extraction

The extraction of basil seeds mucilage was carried out based on a method of Hosseini-Parvar, et al. (2010) with some modifications. The mucilage extraction was performed at 65 $^0$C, pH=8 (0.1 M NaOH and HCl) and water to seed ratio of 50: 1 for 20 min. The seeds were passed through an extractor (Pars Khazar P700, Iran) with a rotating rough plate that scraped the mucilage layer on the seed surface to separate the mucilage from swollen seeds. Then the mucilage was collected and the impurities extracted in extraction mucilage were removed by filtering with cloth filter and centrifuging (Hermle Labortechnik GmbH Z 36 HK, Germany) at 12800 g for 20 min at 20 $^0$C. It was then freeze-dried (Dena, Iran) for 24 h at -40 $^0$C. Finally, the samples were kept in plastic bags at room temperature (Hosseini-Parvar *et al.*, 2010; Razavi *et al.*, 2010).

### Optimization and statistical analysis

Formulation of samples was designed based on four independent variables (gelatin percentage of 1 to 3%, mucilage percentage of

0.5 to 1%, oil phase percentage of 0.4 to 0.8%, and pH of 3.3 to 4.2). Box-Behnken design was implemented to evaluate the effect of gelatin percentage, mucilage percentage, oil phase percentage, and pH on physicochemical properties of microcapsules. Twenty five different runs were proposed by Design Expert Software version 7.0.0 (Stat-Ease Inc., Minneapolis, MN) (Table 1). All the independent variables were kept within range. The analysis of variance (ANOVA) was used to identify significant parameters. Differences of $p<0.01$ were regarded to be significant.

**The encapsulation method**

Encapsulation was performed according to Silva, Favaro-Trindade, Rocha, and Thomazini (2012) method with some modifications. An oily dispersion, consisting of 20% $Q_{10}$, was prepared with sunflower oil. It was added to the aqueous solution of gelatin (based on the percentages provided in Table 1 at $40^0$C and agitated in 14000 rpm for 3 min by a homogenizer (Ultra Turex T18, Germany). A 0.1 M NaOH was used to adjust the the pH at 8. Then an aqueous solution of basil seed mucilage (based on the percentages provided in Table 1 was added to the emulsion at 40 $^0$C. The mixture was stirred using a magnetic stirrer (RH basic 2; IKA® Works) for 10 min and 0.1 M HCl was used to adjust the pH. The coacervate particles were formed by decreasing pH. The turbidity and supernatant absorption were determined by spectrophotometer (PG instruments, T60UV, United Kingdom) at 600 nm. The system was kept at 10 $^0$C for 12 h. Then, the supernatant was separated and coacervate was freeze-dried (Dena, Iran) at 40 $^0$C for 24 h. The freeze-dried material was transferred in a glass jar and aluminum foil was used to keep it away from light (Silva *et al.*, 2012).

**Encapsulation efficiency**

To determine encapsulation efficiency (EE) and encapsulation load (EL), hexane extractable surface and total oil in microcapsule were evaluated. To evaluate surface oil, 0.5 g microcapsule powder was added to 5 ml hexane and it was hand shaken for 5 min. The mixture was then centrifuged (SIGMA Laboratory Centrifuge 3-18, Germany) for 5 min at 2000 rpm. The supernatant was attentively accumulated, filtered through Watman 42 paper filter and transferred to a pre-weighted round-bottom flask. Solvent was eliminated by a rotary evaporator (Hei-VAP; Heidolph Instruments GmbH & Co. KG, Schwabach, Germany) at 60 $^0$C. Surface oil was prescribed gravimetrically (Ifeduba & Akoh, 2016).

To evaluate total oil, 2 ml of 5 M HCl was added to 0.5 g of microcapsule powder in order to release the inner oil and it was agitated using a magnetic stirrer (RH basic 2; IKA® Works) at 60 $^0$C for 1 h. the mixture was allowed to react at room temperature and then it was transferred to a decanter and twice extracted with 5 ml hexane. The supernatant was filtered through Watman 42 paper filter and transferred to a pre-weighted round-bottom flask. The solvent was eliminated by a rotary evaporator (Hei-VAP; Heidolph Instruments GmbH & Co. KG, Schwabach, Germany) at $60^0$C. Total oil was measured gravimetrically (Ifeduba *et al.*, 2016). The encapsulation efficiency (%) and encapsulation load (%) were determined based on the following formula (Calderón-Oliver *et al.*, 2017).

$$\text{Encapsulation efficiency (\%)} = \frac{Wt - Ws}{Wt} \times 100 \quad (1)$$

$$\text{Encapsulation load (\%)} = \frac{Wt - Ws}{Wm} \times 100 \quad (2)$$

Where $W_t$ and $W_s$ are the total and surface oil of the microcapsules and $W_m$ is the mass (g) of the microcapsules.

**Characterization of microcapsules**

To observe the morphology of microcapsules by scanning electron microscope (Philips XL30, Poland), a sample was spread on one side of the double-sided adhesive tape and the other side was glued to a special metal plate. The microcapsules were covered in a vacuum chamber with gold atoms (Peng *et al.*, 2014).

The chemical structures of the microcapsules, $Q_{10}$, gelatin and mucilage were

analyzed by infrared spectroscopy in the region from 4000 - 400 $cm^{-1}$ by using a Fourier transform infrared (FTIR) spectrometer (JASCO FT/IR-680 PLUS, China). Samples were mixed with KBr in a ratio of 1:100 before analysis (Butstraen and Salaün, 2014).

Thermal characteristics of the samples were determined using thermal analyzer (SPA 440, Germany). Samples were transferred to the aluminum pan and heated from 25 to 550 °C at a rate of 10 °C/min under nitrogen atmosphere (Rocha-Selmi *et al*., 2013). The OrginPro (2016 64 Bit) software was used to plot the DSC curves.

Milk was chosen as a food matrix to be enriched with $Q_{10}$ loaded microcapsules. A 0.750 g of microcapsules powder was added to 750 ml milk. Ascorbic acid was used in order to avoid possible oxidation. For saponification, 50 ml KOH 50% was added to 50 ml milk and the sample was kept at 80°C using water bath (WB 22; Memmert GmbH & Co. KG, Schwabach, Germany) for 30 minutes with continuous agitation. The solution was transferred to a decanter and twice extracted with 100 ml hexane. The solvent of the transparent layer was evaporated using a rotary vacuum (Hei-VAP; Heidolph Instruments GmbH & Co. KG, Schwabach, Germany) at 50°C. Finally, a certain amount of n-hexane was added to the oil (Escriva *et al*., 2002; Zamarreño *et al*., 1992). A high-performance liquid chromatography (HPLC) system (Shimadzu, Japan) equipped with column (C18-ods) and UV detector (FPD-6AV) was used to measure $Q_{10}$. Detection of the $CoQ_{10}$ was implemented at 275 nm. Methanol and n-hexane (72:28 v/v) were used as the mobile phase with a flow rate of 1 ml/min (Karpińska *et al*., 2006).

## Results and Discussion

### Encapsulation efficiency and load

This is the first study to figure out the possibility of encapsulating coenzyme $Q_{10}$ using gelatin and basil seed mucilage as wall materials by complex coacervation. Microencapsulation by coacervation occurs by the phase separation of a homogeneous polymer solution into polymer-rich and polymer-poor phases (Silva *et al*., 2012).

Gelatin has a high emulsifying activity and can ionize $-NH_3^+$ and $-COO^-$ in the aqueous solution (Yang *et al*., 2015). When oil was added to the aqueous solution of gelatin, oil in water emulsion was created. By adding an aqueous solution of basil seed mucilage and lowering the pH to below the isoelectric point of gelatin, gelatin became positively charged whereas basil seed mucilage, due to containing carboxyl groups, was negatively charged. Thus, coacervates were formed based on the complexation occurring from the mixture of solutions of substances with opposite charges (Yang *et al*., 2015). In order to develop coacervation more efficiently and to create the greatest possible interaction between the polymers, four formulation variables (gelatin percentage, mucilage percentage, oil phase percentage, and pH) that affect the complex coacervation were assessed.

The values of encapsulation efficiency, encapsulation load, turbidity, and supernatant absorbance were given in Table 1. Analysis of variance indicated that the quadratic model with $R^2$ =0.96 was adequate for predicting encapsulation efficiency (Table 2). The selected model was significant and gelatin concentration, mucilage concentration and oil content had significant effects on encapsulation efficiency ($P<0.01$). Coefficient estimate is a yardstick for comparing the effect of corresponding term in relation to other terms in the model (Saeidy *et al*., 2014). The highest effect on encapsulation efficiency was related to gelatin percentage because it had the maximum coefficient estimate (Table 2). Equation (3) represents experimental model for predicting encapsulation efficiency. The positive coefficients show the increasing and the negative ones show the decreasing effects of model terms on encapsulation efficiency. Therefore, mucilage percentage had an increasing effect and oil phase percentage had a decreasing effect on encapsulation efficiency.

EE (%) = 9.3370+9.0433A+42.61347B+37.07401C–

$$47.82858D+1.93AB+1.13333AC+9.42375AD+0.31556BC-0.1100BD-5.55833CD-3.77616A^2-25.35653B^2-5.06374C^2+15.56792D^2 \quad (3)$$

Where A, B, C and D are gelatin percentage, basil seed mucilage percentage, pH and oil phase percentage, respectively.

**Table 1- The average values of encapsulation efficiency, encapsulation load, turbidity and supernatant absorbance for designed RSM**

| Run | Gelatin percentage | Mucilage percentage | Oil phase percentage | pH | Encapsulation efficiency (%) | Encapsulation load (%) | Turbidity | Supernatant absorbance |
|---|---|---|---|---|---|---|---|---|
| 1 | 2 | 1 | 0.6 | 4.2 | 84.12 | 14.02 | 0.95 | 0.388 |
| 2 | 3 | 0.75 | 0.8 | 3.75 | 82.61 | 14.53 | 0.993 | 0.456 |
| 3 | 2 | 0.75 | 0.8 | 3.3 | 81.11 | 18.28 | 0.951 | 0.269 |
| 4 | 2 | 0.75 | 0.6 | 3.75 | 86.13 | 15.43 | 0.962 | 0.237 |
| 5 | 2 | 0.5 | 0.4 | 3.75 | 87.91 | 12.12 | 0.906 | 0.349 |
| 6 | 3 | 0.75 | 0.6 | 3.3 | 85.04 | 11.73 | 0.97 | 0.488 |
| 7 | 2 | 0.75 | 0.8 | 4.2 | 78.34 | 17.65 | 0.925 | 0.362 |
| 8 | 3 | 1 | 0.6 | 3.75 | 89.5 | 11.67 | 1.016 | 0.411 |
| 9 | 2 | 0.75 | 0.6 | 3.75 | 86.37 | 15.47 | 0.965 | 0.24 |
| 10 | 1 | 0.75 | 0.6 | 3.3 | 78.87 | 20.14 | 0.842 | 0.198 |
| 11 | 2 | 1 | 0.4 | 3.75 | 93.13 | 10.96 | 0.976 | 0.217 |
| 12 | 3 | 0.75 | 0.6 | 4.2 | 84.9 | 11.71 | 0.956 | 0.594 |
| 13 | 1 | 0.75 | 0.4 | 3.75 | 86.15 | 16.03 | 0.88 | 0.172 |
| 14 | 3 | 0.5 | 0.6 | 3.75 | 83.26 | 12.18 | 0.975 | 0.501 |
| 15 | 2 | 0.75 | 0.6 | 3.75 | 85.98 | 15.4 | 0.964 | 0.231 |
| 16 | 2 | 1 | 0.8 | 3.75 | 82.51 | 17.37 | 0.987 | 0.235 |
| 17 | 1 | 0.75 | 0.6 | 4.2 | 76.69 | 19.58 | 0.831 | 0.272 |
| 18 | 1 | 0.75 | 0.8 | 3.75 | 66.51 | 20.87 | 0.87 | 0.181 |
| 19 | 2 | 0.5 | 0.8 | 3.75 | 77.31 | 18.74 | 0.933 | 0.361 |
| 20 | 2 | 0.5 | 0.6 | 4.2 | 80.21 | 15.52 | 0.878 | 0.422 |
| 21 | 3 | 0.75 | 0.4 | 3.75 | 94.71 | 9.13 | 0.983 | 0.432 |
| 22 | 2 | 0.75 | 0.4 | 4.2 | 90.34 | 11.47 | 0.917 | 0.337 |
| 23 | 2 | 1 | 0.6 | 3.3 | 85.8 | 14.3 | 0.956 | 0.242 |
| 24 | 1 | 0.5 | 0.6 | 3.75 | 72 | 20.57 | 0.851 | 0.161 |
| 25 | 1 | 1 | 0.6 | 3.75 | 76.31 | 17.61 | 0.901 | 0.212 |
| 26 | 2 | 0.5 | 0.6 | 3.3 | 82.03 | 15.88 | 0.886 | 0.365 |
| 27 | 2 | 0.75 | 0.6 | 3.75 | 85.47 | 15.31 | 0.959 | 0.245 |
| 28 | 2 | 0.75 | 0.4 | 3.3 | 91.11 | 11.57 | 0.937 | 0.271 |
| 29 | 2 | 0.75 | 0.6 | 3.75 | 85.13 | 15.25 | 0.96 | 0.249 |
| | | | | Standard error | 1.14 | 0.59 | 0.009 | 0.021 |

Wall to core ratio is an important factor in the final characteristics of the microcapsules (Hogan *et al*., 2001). Fig. 1 (A) shows the interaction of gelatin and mucilage concentrations on encapsulation efficiency. Increasing of wall materials led to enhance of encapsulation efficiency due to more available space for coenzyme Q10 to be entrapped. According to Fig. 1 (B), increasing of oil percentage from 0.4% to 0.8% resulted in a decrease in the encapsulation efficiency from 90.23% to 80.36%, which could be due to the shortage of wall materials for oil entrapment. Xiao *et al.* (2015) encapsulated styralyl acetate (SA) using gelatin and gum Arabic with complex coacervation method. They indicated that when the amount of SA remained 1.0 g and wall concentration increased from 0.5 to 1.3 %, encapsulation efficiency enhanced from 23 to 57 % (Xiao *et al*., 2015).

A

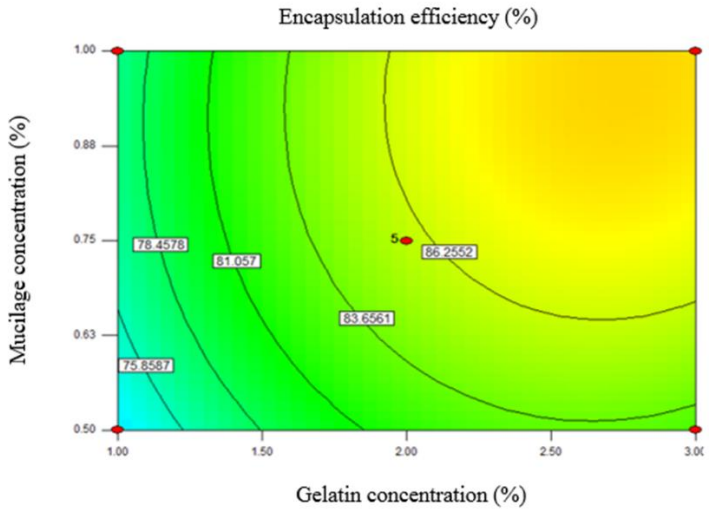


B

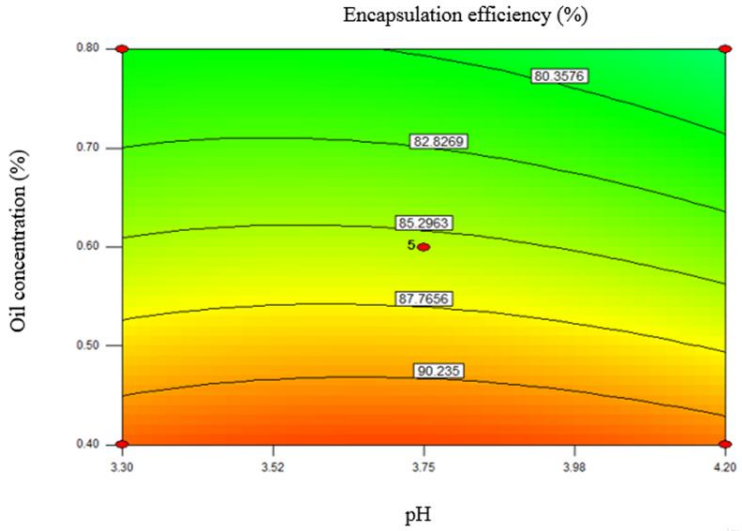


**Fig. 1- Interaction of gelatin and mucilage concentrations (%) (A) and oil concentration (%) and pH (B) on encapsulation efficiency**

Quadratic model with $R^2$=0.99 was appropriate to state encapsulation load (Table 2). Among the four independent variables, only pH had no significant effect on encapsulation load (P<0.01). According to Table 2, oil phase percentage had the highest coefficient in relation to other terms in the model.

EL (%) =8.51077-8.5565A-2.71435B+3.69399C+34.82916D+2.45061AB +0.29882AC+0.69747AD+0.16143BC-1.01307BD-1.46298CD+0.38153$A^2$-3.47631$B^2$-0.51904$C^2$-12.42667$D^2$ (4)

Where A, B, C and D are gelatin percentage, basil seed mucilage percentage, pH and oil phase percentage, respectively.

**Table 2- Model parameters for the quadratic equation for prediction of encapsulation efficiency, encapsulation load, turbidity and supernatant absorbance**

| Source | Encapsulation efficiency ($R^2$=0.96 ) | | Encapsulation load ($R^2$=0.99) | | Turbidity ($R^2$=0.99) | | Supernatant absorbance ($R^2$=0.97) | |
|---|---|---|---|---|---|---|---|---|
| | Coefficient estimate | P | Coefficient estimate | P | Coefficient estimate | P | Coefficient estimate | P |
| Model | 85.82 | < 0.0001 | 15.37 | <0. 0001 | 0.96 | < 0.0001 | 0.24 | < 0.0001 |
| A | 5.29 | < 0.0001 | -3.65 | < 0.0001 | 0.06 | < 0.0001 | 0.14 | <0.0001 |
| B | 2.39 | 0.0002 | -0.76 | < 0.0001 | 0.03 | < 0.0001 | -0.038 | 0.0002 |
| C | -0.78 | 0.1253 | -0.16 | 0.2366 | 0 | 0.0193 | 0.045 | < 0.0001 |
| D | -6.25 | < 0.0001 | 3.01 | < 0.0001 | 0 | 0.0973 | 0 | 0.3635 |
| AB | 0.48 | 0.5702 | 0.61 | 0.0167 | 0 | 0.6154 | -0.035 | 0.0184 |
| AC | 0.51 | 0.5487 | 0.13 | 0.5607 | 0 | 0.9309 | 0 | 0.5546 |
| AD | 1.88 | 0.0394 | 0.14 | 0.5463 | 0 | 0.3045 | 0 | 0.7807 |
| BC | 0.036 | 0.9665 | 0.018 | 0.9370 | 0 | 0.9284 | 0.022 | 0.1144 |
| BD | 0 | 0.9948 | -0.051 | 0.8256 | 0 | 0.4156 | 0 | 0.9112 |
| CD | -0.5 | 0.5562 | -0.13 | 0.5687 | 0 | 0.7534 | 0 | 0.6175 |
| A2 | -3.78 | < 0.0001 | 0.38 | 0.0492 | -0.025 | <0.0001 | 0.061 | <0.0001 |
| B2 | -1.58 | 0.029 | -0.22 | 0.2403 | 0 | 0.0736 | 0.034 | 0.0057 |
| C2 | -1.03 | 0.1379 | -0.11 | 0.5624 | -0.034 | < 0.0001 | 0.077 | < 0.0001 |
| D2 | 0.62 | 0.3555 | -0.5 | 0.014 | 0 | 0.6294 | 0 | 0.5692 |

Fig. 2 (A) showed that in the constant concentration of oil, encapsulation load decreased from 19.09% to 13.21 % as wall materials concentration increased. Encapsulation load is the ratio of loaded $CoQ_{10}$ to the weight of the final microcapsule; thus, the low EL can be ascribed to the thick wall of the capsules formed. By increasing the oil content, encapsulation load increased from 12.78% to 17.02 % due to the fact that wall materials were able to encapsulate more amount of oil (Fig. 2 (B). The result was similar from what was reported by Ahmadi *et al*. (2015) who applied β-Lactoglobulin/Arabic Gum complex coacervation. When the encapsulation load is low, the microcapsules have a larger wall thickness which ensures better protection of their core against environmental factors. However, high loading lead to placement of the core near the surface of the wall which results in a faster release to the surrounding environment (Calderón-Oliver *et al*., 2017).

## Turbidity and supernatant absorbance

Turbidity and supernatant absorbance are reliable parameters to be taken into account when optimizing the complex coacervation process (Chang *et al*., 2016). Quadratic model with $R^2$=0.99 was suggested to explain turbidity (Table 2). Gelatin percentage and mucilage percentage had significant effects on turbidity (P<0.01). Equation (5) shows descriptive model for turbidity.

$$\text{Turbidity} = -1.81075+0.15696A+0.34321B+1.25882C+0.15102D-0.0096899AB-0.000925271AC+0.025128AD+0.00383722BC-0.079112BD-0.016786CD-0.025398A^2-0.11457B^2-0.16877C^2-0.045673D^2 \quad (5)$$

Where A, B, C and D are gelatin percentage, basil seed mucilage percentage, pH and oil phase percentage, respectively.

Turbidimetric assay enables visual evaluation of the behavior of polymers during complexation and simplifies the verification of complex formation (Prata and Grosso, 2015). The higher turbidity is desirable since it shows that more electrostatic complexes are formed. Fig. 3 (A) demonstrated that by decreasing the pH from 4.2 to 3.75, the turbidity increased that indicating the formation of dense microcapsules. A further decrease in the pH from about 3.75 to 3.3 led to lower turbidity that representing the low number of electrostatic complexes. The ionization degree of active groups dependents on solution's pH and in an effective pH, opposite charges are available which causes to their interaction (Jun-xia *et al*.,

2011). Similar results have been reported by Wang *et al.* for microencapsulation of tuna oil in gelatin- sodium hexametaphosphate using complex coacervation (Wang *et al.*, 2014).

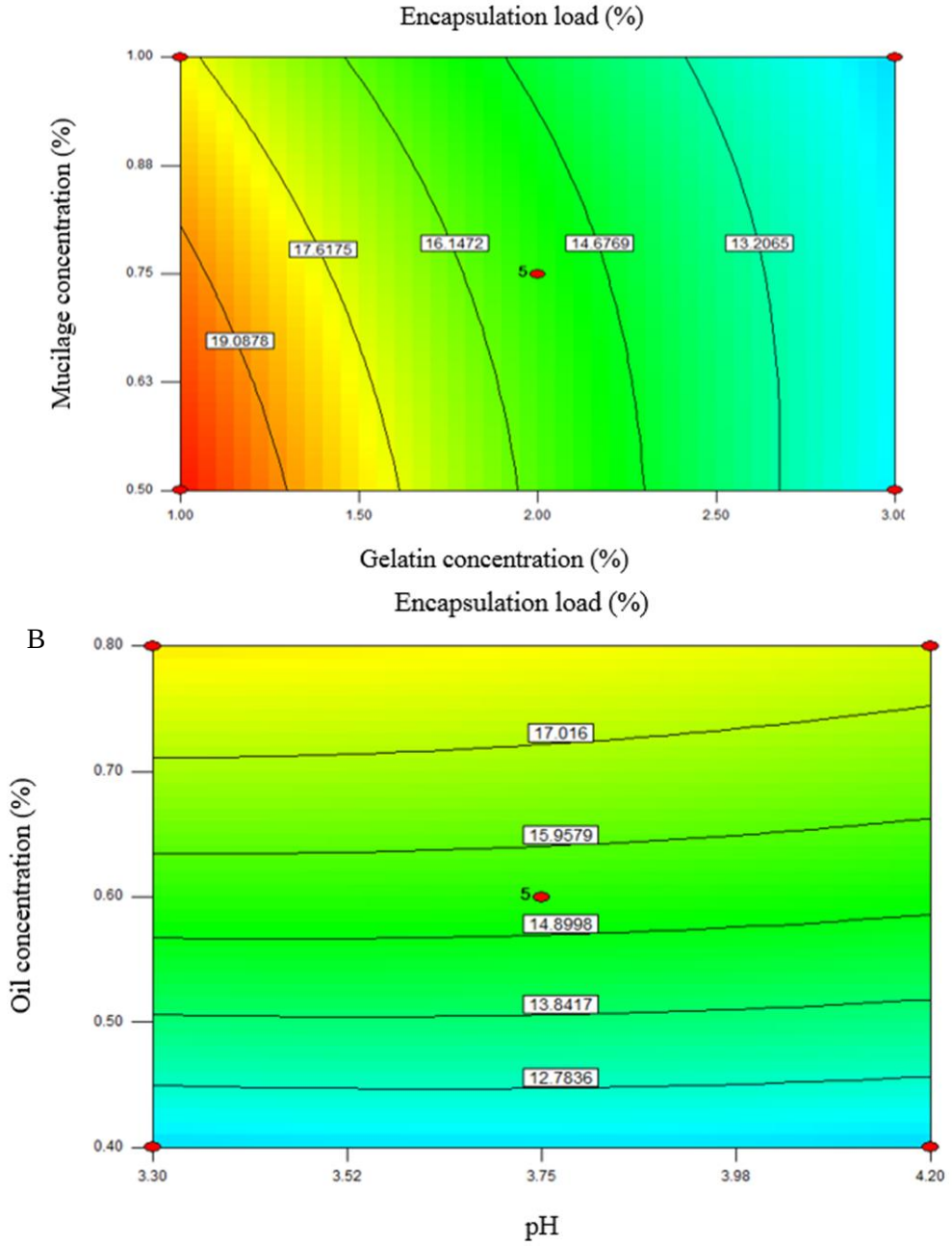


**Fig. 2- Interaction of gelatin and mucilage concentrations (%) (A) and oil concentration (%) and pH (B) on encapsulation load**

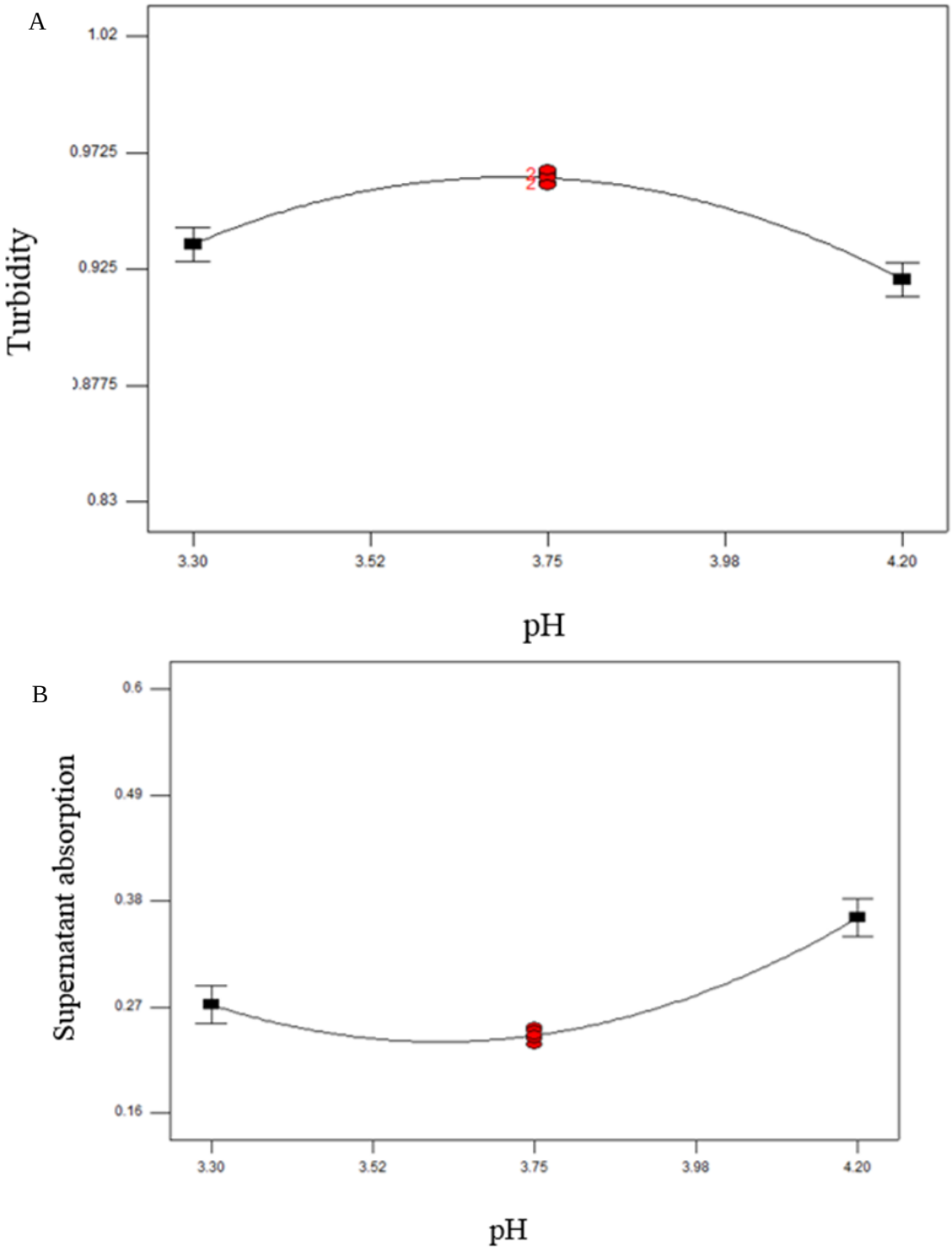


**Fig. 3- Effect of pH on turbidity (A) and supernatant absorption (B) of solution**

Analysis of variance indicated that the quadratic model with $R^2$ =0.97 was suitable to predict supernatant absorbance (Table 2). Gelatin percentage, mucilage percentage and pH had significant effects on supernatant absorbance ($P<0.01$). Equation (6) shows selected model for supernatant absorbance:

Supernatant absorbance =6.29203-0.073867A-1.44020B-2.97296C-0.48692D-0.14100AB+0.017778AC+0.018750 AD+0.19778BC+0.03BD+0.075CD+0.060550 $A^2$+0.54080$B^2$+0.37926$C^2$+0.15125$D^2$ (6)

where A, B, C and D are gelatin percentage, basil seed mucilage percentage, pH and oil phase percentage, respectively.

Lower the absorption is desirable since it represents that higher solid materials are in coacervate phase. Fig. 3 (B) demonstrated the effect of pH on supernatant absorption and indicated that by decreasing pH to 3.75, the absorption of the supernatant phase decreased, which showed more wall materials interacted and formed coacervate. A further decrease in pH range from about 3.75 to 3.3 led to higher absorption of the supernatant phase, indicating the low number of complexes in coacervate phase. The complex coacervation is significantly affected by pH of the solution. Jun-xia *et al*. (2011) used soy protein isolate and gum Arabic to encapsulate orange oil and reported that pH 4 is the electrical equivalence point. The charge densities of the two biopolymers were in stoichiometric equilibrium at pH 4 and therefore pH 4 had the highest coacervate yield.

**Response surface optimization**

The optimal formula was selected using the Design Expert software based on the highest percentage of encapsulation efficiency, encapsulation load, turbidity and lowest supernatant absorbance. The optimal formula with gelatin concentration of 2.02%, mucilage concentration of 0.91%, oil phase concentration of 0.71% and pH of 3.61 had encapsulation efficiency, encapsulation load, turbidity and supernatant absorbance of 83.69%, 16.32%, 0.979 and 0.227, respectively. Minor differences were observed between RSM data and our laboratory data. The optimum sample was selected to investigate the morphology, chemical structure and thermal behavior of microcapsules.

**Characterization of microcapsules**

Fig. 4 (A) shows a microscopic image of the $Q_{10}$ loaded in the microcapsules after drying. The microcapsules were generally spherical and had rugged surfaces. These microcapsules stuck to each other because of the interaction of free oil and wall materials on the surface of the particles, which had not participated in complex coacervation process. The same result was reported by Yari *et al.* (2016). The presence of holes in the surface might due to the use of freeze dryer to dry the microcapsules. The removal of ice particles by sublimation leads to open holes (Fonte *et al*., 2012).

Fig. 4 (B) shows the IR spectra of gelatin, basil seed mucilage, sunflower oil, $COQ_{10}$ and microcapsules. The IR spectrum of gelatin had a strong band at 3423 $cm^{-1}$, which was related to the N-H stretching vibrations. Weak peaks at 2921 $cm^{-1}$ and 1450 $cm^{-1}$ were attributed to the stretching and bending vibrations of C-H, respectively. Also, weak peaks at 1240 $cm^{-1}$ and 1079 $cm^{-1}$ were attributed to the C-N bending vibrations. The strong peak at 1638 $cm^{-1}$ was related to the stretching vibrations of the carbonyl group (C=O) of amide I. The peak at 1546 $cm^{-1}$ indicated the bending mods of N-H bond of amid II. The peak at 1202 $cm^{-1}$ was attributed to the vibrations of N-H and C-N groups of amide III (Duhoranimana *et al*., 2017).

The IR spectrum of mucilage, showed different peaks at 3419 $cm^{-1}$, 2919 $cm^{-1}$, 1603 $cm^{-1}$, 1416 $cm^{-1}$ and 1046 were assigned to OH, $CH_2$, C-OO asymmetric stretching, C-OO symmetric stretching and C-O-C stretching, respectively (Naji-Tabasi *et al*., 2016).

In the spectrum of sunflower oil, peaks at 2924 $cm^{-1}$, 2854 $cm^{-1}$, 1747 $cm^{-1}$ ، 1654 $cm^{-1}$ were attributed to the -CH asymmetric stretching, -CH symmetric stretching, -CO stretching vibrations and -C-C- stretching vibrations, respectively. The peak at 1163 $cm^{-1}$ was assigned to the stretching and bending vibrations of -C-O and $CH_2$. Band at 723 $cm^{-1}$ reflected the bending vibrations of -HC-CH- and - $(CH2)_n$-. The peak at 3471 $cm^{-1}$ presented the overtone of -C-O ester. The -C-H stretching

vibrations at 3008 $cm^{-1}$ and the bending vibrations of -C-H at 1463 $cm^{-1}$ were other major peaks of the sunflower oil spectrum (Hamed and Allam, 2006).

In the spectrum of $CoQ_{10}$, the peaks at 2950 $cm^{-1}$, 2843 $cm^{-1}$ and 1605 $cm^{-1}$ were assigned to the stretching vibrations of =CH, -CH3 and carbonyl (-C=O), respectively. The stretching vibrations of the methoxy group at 1382 $cm^{-1}$ and the ether group at 1266 $cm^{-1}$ were other peaks of the $CoQ_{10}$ spectrum (Akhter *et al.*, 2014).

The peaks of the microcapsule spectrum showed the main peaks of ingredients. While, peaks at 1546 $cm^{-1}$ of gelatin spectrum and 1416 $cm^{-1}$ of the basil mucilage spectrum were not detectable. A new peak appeared at 1490 $cm^{-1}$, indicating the formation of ionic interaction between the negative carboxyl group of the mucilage and the protonated amine group of gelatin. Presence of coenzyme $Q_{10}$ bands was a reason supporting encapsulation of coenzyme $Q_{10}$ by mucilage-gelatin microparticles. The sametrend was reported by Kavousi *et al.* (2017) for encapsulation of fish oil in hydrogels of cress seed mucilage and chitosan (Kavousi *et al.*, 2017).

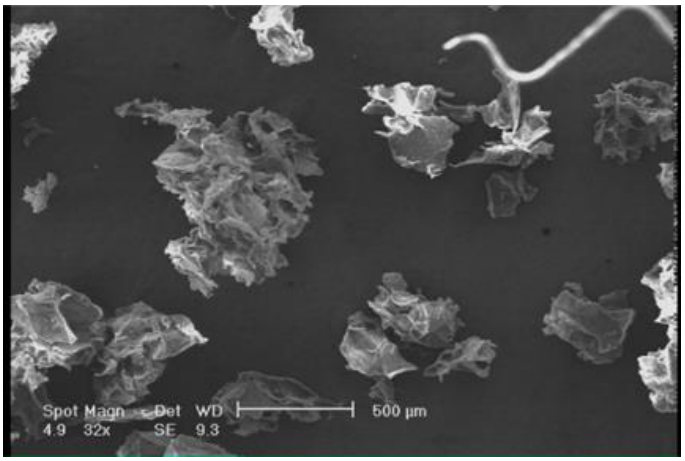

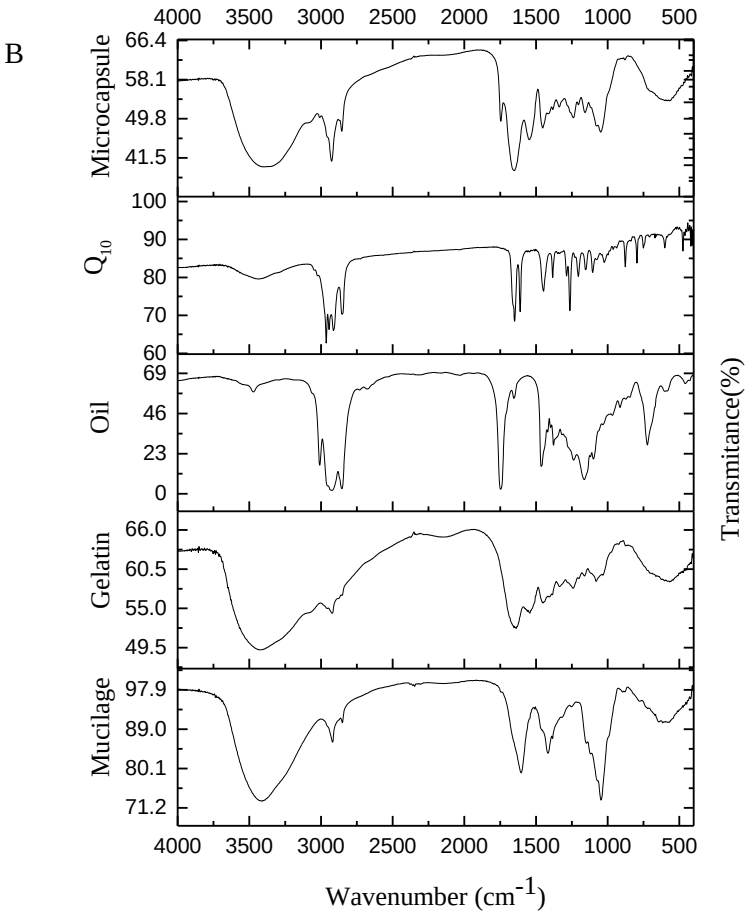


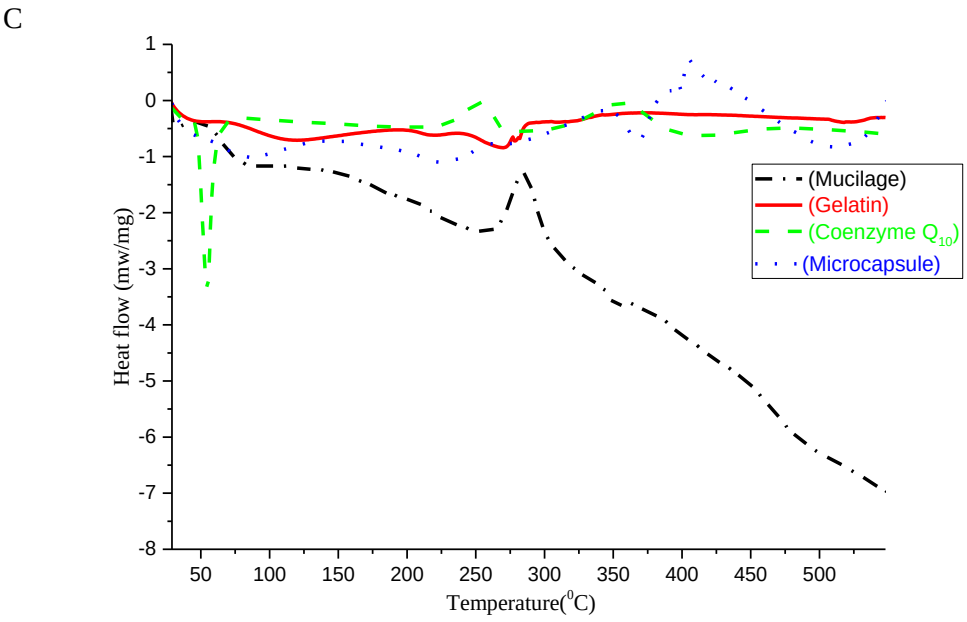


**Fig. 4- SEM image of Q10 loaded microcapsules (A), FTIR spectra (B) and DSC curves (C) of ingredients and produced microcapsules**

Fig. 4 (C) shows DSC curves of gelatin, mucilage, $CoQ_{10}$, and microcapsule. The glass transition (Tg) of gelatin was at 70°C. The peaks at 110 and 280°C represented melting point and decomposition of gelatin (Li *et al.*, 2006; Rahman *et al.*, 2010). The endothermic peaks at 47°C and 90°C represent glass transition temperature and water evaporation in basil mucilage, respectively (Khazaei *et al.*, 2014). The melting point of $CoQ_{10}$ at 50°C indicated its crystalline nature (Swarnakar *et al.*, 2011). For the thermogram of $Q_{10}$ loaded microcapsule, melting point was not observed at 50 °C due to its solubility in the oil phase and appropriate entrapment (Gokce *et al.*, 2012). The mucilage melting points and the glass transition point of gelatin were observed in the microcapsule's thermal curve. The peak at 350 °C could be attributed to the microcapsule decomposition temperature. The microcapsule had the higher thermal resistance in comparison to other ingredients due to interaction of wall materials. Kavousi *et al.* (2017) studied microencapsulation of fish oil in hydrogels of cress seed mucilage (CSM) and chitosan (CS) and reported that the thermal resistance of CSM/CS hydrogel loaded with fish oil was significantly higher than CSM and CS (Kavousi *et al.*, 2017).

Liposoluble vitamins in milk were taken up during the hexane-extraction process. $CoQ_{10}$ shows its characteristic maxima of UV absorption at 275 nm. This analytical wavelength was selected for the HPLC-UV detection to enhance the selectivity and sensitivity of analysis (Karpińska *et al.*, 2006). In order to study the release of $CoQ_{10}$ from microcapsules in milk, its amount was analyzed during storage at 4°C. About 4.2% and 12.4% of total added $CoQ_{10}$ released in milk for the 1$^{st}$ and 5$^{th}$ days of storage, respectively. The release rate of $CoQ_{10}$ from microcapsules was high at the beginning of storage because of $CoQ_{10}$ distributed on the surface or surface layer which was easier to release. The first release followed with slower release because of $CoQ_{10}$ in microcapsule mainly released through the microcapsules wall by swelling and diffusion. Jain *et al.* (2015) studied release of β-Carotene from whey protein isolates/gum acacia complex and reported the same issue (Jain *et al.*, 2015).

## Conclusion

A new set of wall materials was applied to prepare microcapsules. Basil seed mucilage, an anionic polysaccharide was able to build complex and form coacervates with gelatin via electrostatic interaction under specific conditions. The efficiency of encapsulation increased as the higher wall materials were used under conditions where the core material in the system was kept constant. The optimal formula with gelatin concentration of 2.02%, mucilage concentration of 0.91%, oil phase concentration of 0.71% and pH of 3.61 was determined. The microcapsules were generally spherical and had rugged surfaces. FTIR spectra revealed that ionic interactions occurred between functional groups of gelatin and basil seed mucilage. The thermal stability of coacervate showed that basil seed mucilage- gelatin coacervate will be appropriate to be used for encapsulation of thermally sensitive materials. The results of this study indicated that the produced microcapsules can be used to encapsulate and control the release of bioactive ingredients. Further studies should be performed toward the stability of microcapsules in different food media and their large scale production.

## References

1. Ahmadi, N., Nasirpour, A., Sheikhzeinodin, M., & Keramat, J. (2015). Microencapsulation of ubiquinone using complex coacervation for functional yoghurt. *Food Science and BiotechnologyBiochimica et Biophysica Acta (BBA)-Molecular Basis of Disease, 24*(3), 895-904. http://dx.doi.org/10.1007/s10068-015-0116-x

2. Akhter, M.H., Ahmad, A., Ali, J., & Mohan, G. (2014). Formulation and development of $CoQ_{10}$-loaded s-SNEDDS for enhancement of oral bioavailability. *Journal of Pharmaceutical Innovation*, *9*(2), 121-131. http://dx.doi.org/10.1007/s12247-014-9179-0
3. Butstraen, C., & Salaün, F. (2014). Preparation of microcapsules by complex coacervation of gum Arabic and chitosan. *Carbohydrate Polymers*, *99*, 608-616. https://doi.org/10.1016/j.carbpol.2013.09.006
4. Byeon, J.H., Kang, Y.-R., & Chang, Y.H. (2023). Physicochemical and in vitro digestion properties of gelatin/low-methoxyl pectin synbiotic microgels co-encapsulating Lacticaseibacillus casei and pectic oligosaccharides via double-crosslinking with transglutaminase and calcium ions. *Food Hydrocolloids*, *142*, 108757. https://doi.org/10.1016/j.foodhyd.2023.108757
5. Calderón-Oliver, M., Pedroza-Islas, R., Escalona-Buendía, H.B., Pedraza-Chaverri, J., & Ponce-Alquicira, E. (2017). Comparative study of the microencapsulation by complex coacervation of nisin in combination with an avocado antioxidant extract. *Food Hydrocolloids*, *62*, 49-57. https://doi.org/10.1016/j.foodhyd.2016.07.028
6. Chang, P.G., Gupta, R., Timilsena, Y.P., & Adhikari, B. (2016). Optimisation of the complex coacervation between canola protein isolate and chitosan. *Journal of Food Engineering*, *191*, 58-66. https://doi.org/10.1016/j.jfoodeng.2016.07.008
7. Dong, Z., Ma, Y., Hayat, K., Jia, C., Xia, S., & Zhang, X. (2011). Morphology and release profile of microcapsules encapsulating peppermint oil by complex coacervation. *Journal of Food Engineering*, *104*(3), 455-460. https://doi.org/10.1016/j.jfoodeng.2011.01.011
8. Duhoranimana, E., Karangwa, E., Lai, L., Xu, X., Yu, J., Xia, S., Zhang, X., Muhoza, B., & Habinshuti, I. (2017). Effect of sodium carboxymethyl cellulose on complex coacervates formation with gelatin: Coacervates characterization, stabilization and formation mechanism. *Food Hydrocolloids*, *69*, 111-120. https://doi.org/10.1016/j.foodhyd.2017.01.035
9. Escriva, A., Esteve, M., Farré, R., & Frıgola, A. (2002). Determination of liposoluble vitamins in cooked meals, milk and milk products by liquid chromatography. *Journal of Chromatography A*, *947*(2), 313-318. https://doi.org/10.1016/S0021-9673(01)01618-1
10. Fonte, P., Soares, S., Costa, A., Andrade, J. C., Seabra, V., Reis, S., & Sarmento, B. (2012). Effect of cryoprotectants on the porosity and stability of insulin-loaded PLGA nanoparticles after freeze-drying. *Biomatter*, *2*(4), 329-339. https://doi.org/10.4161/biom.23246
11. Gokce, E.H., Korkmaz, E., Tuncay-Tanrıverdi, S., Dellera, E., Sandri, G., Bonferoni, M.C., & Ozer, O. (2012). A comparative evaluation of coenzyme Q10-loaded liposomes and solid lipid nanoparticles as dermal antioxidant carriers. *International Journal of Nanomedicine*, *7*, 5109. https://doi.org/10.2147/ijn.s34921
12. Hamed, S., & Allam, M.A. (2006). Application of FTIR spectroscopy in the determination of antioxidant efficiency in sunflower oil. *Journal of Applied Sciences Research*, *2*(1), 27-33.
13. Hogan, S.A., McNamee, B.F., O'Riordan, E.D., & O'Sullivan, M. (2001). Microencapsulating properties of sodium caseinate. *Journal of Agricultural and Food Chemistry*, *49*(4), 1934-1938. https://doi.org/10.1021/jf000276q
14. Hosseini-Parvar, S., Matia-Merino, L., Goh, K., Razavi, S.M.A., & Mortazavi, S.A. (2010). Steady shear flow behavior of gum extracted from *Ocimum basilicum* L. seed: effect of concentration and temperature. *Journal of Food Engineering*, *101*(3), 236-243. https://doi.org/10.1016/j.jfoodeng.2010.06.025
15. Hu, R., Dong, D., Hu, J., & Liu, H. (2023). Improved viability of probiotics encapsulated in soybean protein isolate matrix microcapsules by coacervation and cross-linking modification. *Food Hydrocolloids*, *138*, 108457. https://doi.org/10.1016/j.foodhyd.2023.108457

16. Ifeduba, E.A., & Akoh, C.C. (2016). Microencapsulation of stearidonic acid soybean oil in Maillard reaction-modified complex coacervates. *Food Chemistry, 199*, 524-532. https://doi.org/10.1016/j.foodchem.2015.12.011
17. Jain, A., Thakur, D., Ghoshal, G., Katare, O., & Shivhare, U. (2015). Microencapsulation by complex coacervation using whey protein isolates and gum acacia: an approach to preserve the functionality and controlled release of β-carotene. *Food and Bioprocess Technology, 8*(8), 1635-1644. http://dx.doi.org/10.1007/s11947-015-1521-0
18. Jun-xia, X., Hai-yan, Y., & Jian, Y. (2011). Microencapsulation of sweet orange oil by complex coacervation with soybean protein isolate/gum Arabic. *Food Chemistry, 125*(4), 1267-1272. https://doi.org/10.1016/j.foodchem.2010.10.063
19. Karpińska, J., Mikołuć, B., Motkowski, R., & Piotrowska-Jastrzębska, J. (2006). HPLC method for simultaneous determination of retinol, α-tocopherol and coenzyme $Q_{10}$ in human plasma. *Journal of Pharmaceutical and Biomedical Analysis, 42*(2), 232-236. https://doi.org/10.1016/j.jpba.2006.03.037
20. Kavousi, H. R., Fathi, M., & Goli, S. A. (2017). Stability enhancement of fish oil by its encapsulation using a novel hydrogel of cress seed mucilage/chitosan. *International Journal of Food Properties, 20*(sup2), 1890-1900. https://doi.org/10.1080/10942912.2017.1357042
21. Khazaei, N., Esmaiili, M., Djomeh, Z. E., Ghasemlou, M., & Jouki, M. (2014). Characterization of new biodegradable edible film made from basil seed (*Ocimum basilicum* L.) gum. *Carbohydrate Polymers, 102*, 199-206. https://doi.org/10.1016/j.carbpol.2013.10.062
22. Li, M., Guo, Y., Wei, Y., MacDiarmid, A.G., & Lelkes, P.I. (2006). Electrospinning polyaniline-contained gelatin nanofibers for tissue engineering applications. *Biomaterials, 27*(13), 2705-2715. https://doi.org/10.1016/j.biomaterials.2005.11.037
23. Li, X., Zhang, M., Zhou, L., Liu, J., & Marchioni, E. (2023). Construction of whey protein gels prepared by three methods to stabilize high internal phase Pickering emulsions loaded with $CoQ_{10}$ under different pH. *Food Chemistry, 421*, 136192. https://doi.org/10.1016/j.foodchem.2023.136192
24. Naji-Tabasi, S., Razavi, S.M.A., Mohebbi, M., & Malaekeh-Nikouei, B. (2016). New studies on basil (Ocimum bacilicum L.) seed gum: Part I–Fractionation, physicochemical and surface activity characterization. *Food Hydrocolloids, 52*, 350-358. https://doi.org/10.1016/j.foodhyd.2015.07.011
25. Nakagawa, K., & Nagao, H. (2012). Microencapsulation of oil droplets using freezing-induced gelatin–acacia complex coacervation. *Colloids and Surfaces A: Physicochemical and Engineering Aspects, 411*, 129-139. https://doi.org/10.1016/j.colsurfa.2012.07.010
26. Peng, C., Zhao, S.-Q., Zhang, J., Huang, G.-Y., Chen, L.-Y., & Zhao, F.-Y. (2014). Chemical composition, antimicrobial property and microencapsulation of Mustard (Sinapis alba) seed essential oil by complex coacervation. *Food Chemistry, 165*, 560-568. https://doi.org/10.1016/j.foodchem.2014.05.126
27. Prata, A.S., & Grosso, C.R. (2015). Influence of the oil phase on the microencapsulation by complex coacervation. *Journal of the American Oil Chemists' Society, 92*(7), 1063-1072. http://dx.doi.org/10.1007/s11746-015-2670-z
28. Rahman, M. S., Al-Saidi, G., Guizani, N., & Abdullah, A. (2010). Development of state diagram of bovine gelatin by measuring thermal characteristics using differential scanning calorimetry (DSC) and cooling curve method. *Thermochimica Acta, 509*(1-2), 111-119. https://doi.org/10.1016/j.tca.2010.06.011.

29. Razavi, S.M., Bostan, A., & Rezaie, M. (2010). Image processing and physico-mechanical properties of basil seed (*Ocimum basilicum*). *Journal of Food Process Engineering, 33*(1), 51-64. https://doi.org/10.1111/j.1745-4530.2008.00259.x
30. Rocha-Selmi, G.A., Theodoro, A.C., Thomazini, M., Bolini, H.M., & Favaro-Trindade, C.S. (2013). Double emulsion stage prior to complex coacervation process for microencapsulation of sweetener sucralose. *Journal of Food Engineering, 119*(1), 28-32. https://doi.org/10.1016/j.jfoodeng.2013.05.002.
31. Saeidy, S., Keramat, J., & Nasirpour, A. (2014). Microencapsulation of calcium using water-in-oil-in-water double emulsion method. *Journal of Dispersion Science and Technology, 35*(3), 370-379. https://doi.org/10.1080/01932691.2013.788453
32. Sharifi, S., Rezazad-Bari, M., Alizadeh, M., Almasi, H., & Amiri, S. (2021). Use of whey protein isolate and gum Arabic for the co-encapsulation of probiotic Lactobacillus plantarum and phytosterols by complex coacervation: Enhanced viability of probiotic in Iranian white cheese. *Food Hydrocolloids, 113*, 106496. https://doi.org/10.1016/j.foodhyd.2020.106496.
33. Silva, D., Favaro-Trindade, C., Rocha, G., & Thomazini, M. (2012). Microencapsulation of lycopene by gelatin–pectin complex coacervation. *Journal of Food Processing and Preservation, 36*(2), 185-190. https://doi.org/10.1111/j.1745-4549.2011.00575.x.
34. Swarnakar, N.K., Jain, A.K., Singh, R.P., Godugu, C., Das, M., & Jain, S. (2011). Oral bioavailability, therapeutic efficacy and reactive oxygen species scavenging properties of coenzyme Q10-loaded polymeric nanoparticles. *Biomaterials, 32*(28), 6860-6874. https://doi.org/10.1016/j.biomaterials.2011.05.079.
35. Wang, B., Adhikari, B., & Barrow, C.J. (2014). Optimisation of the microencapsulation of tuna oil in gelatin–sodium hexametaphosphate using complex coacervation. *Food Chemistry, 158*, 358-365. https://doi.org/10.1016/j.foodchem.2014.02.135
36. Wang, C., Zhao, R., He, K., Zhang, S., Kemp, A.H., & Guo, M. (2023). Pharmacokinetic profile and sub-chronic toxicity of coenzyme Q10 loaded whey protein nanoparticles. *Food Bioscience, 52*, 102347. https://doi.org/10.1016/j.fbio.2022.102347
37. Xiao, Z., Li, W., & Zhu, G. (2015). Effect of wall materials and core oil on the formation and properties of styralyl acetate microcapsules prepared by complex coacervation. *Colloid and Polymer Science, 293*(5), 1339-1348.
38. Yang, X., Gao, N., Hu, L., Li, J., & Sun, Y. (2015). Development and evaluation of novel microcapsules containing poppy-seed oil using complex coacervation. *Journal of Food Engineering, 161*, 87-93. https://doi.org/10.1016/j.jfoodeng.2015.03.027
39. Yari, S., Nasirpour, A., & Fathi, M. (2016). Effect of polymer concentration and acidification time on olive oil microcapsules obtained by complex coacervation. *Applied Food Biotechnology, 3*(1), 53-58. http://dx.doi.org/10.22037/afb.v3i1.10226
40. Zamarreño, M.D., Pérez, A.S., Pérez, C.G., & Méndez, J.H. (1992). High-performance liquid chromatography with electrochemical detection for the simultaneous determination of vitamin A, D3 and E in milk. *Journal of Chromatography A, 623*(1), 69-74. https://doi.org/10.1016/0021-9673(92)85300-I

نشریه پژوهشهای علوم و صنایع غذایی ایران
جلد ۱۹، شماره ۳، مرداد- شهریور ۱۴۰۲ ص. ۳۱-۱۵

Iranian Food Science and Technology Research Journal
Vol. 19, No. 3, Aug.-Sep. 2023, p. 15-31

# ریزپوشینه کردن کوآنزیم $Q_{10}$ به روش توده‌سازی مرکب ژلاتین و موسیلاژ دانه ریحان: بهینه‌سازی، ویژگی‌های فیزیکوشیمیایی و غنی‌سازی شیر

ستاره رمضانی[۱]- محمد شاهدی[۲]- میلاد فتحی[۳*]

تاریخ دریافت: ۱۴۰۱/۱۲/۲۶
تاریخ بازنگری۱۴۰۲/۰۳/۲۴
تاریخ پذیرش: ۱۴۰۲/۰۴/۰۷

## چکیده

نگرانی جهانی در مورد سلامت انسان و افزایش شیوع بیماری‌های مزمن در سال‌های اخیر منجر به افزایش تقاضا برای ترکیبات مغذی مانند کوآنزیم $Q_{10}$ شده است. حساسیت به گرما و خواص چربی دوست کوآنزیم $Q_{10}$ استفاده از آن را در غذا محدود می‌کند. کپسولاسیون فناوری است که از مواد زیست فعال در برابر شرایط محیطی نامناسب محافظت می‌کند و عمر مفید را افزایش می‌دهد. هدف از این مطالعه کپسوله‌سازی کوآنزیم $Q_{10}$ با استفاده از کواسرواسیون مرکب توسط موسیلاژ دانه ژلاتین-ریحان و مشخص کردن خواص فیزیکی، حرارتی و شیمیایی میکروکپسول‌های تولید شده بود. روش سطح پاسخ برای تعیین سطح بهینه چهار متغیر فرمولاسیون برای حداکثر راندمان کپسولاسیون، ظرفیت بارگذاری و کدورت و حداقل جذب مایع رویی استفاده شد. میکروکپسول‌های بهینه دارای راندمان کپسولاسیون ۸۳/۶۹٪، ظرفیت بارگذاری ۱۶/۳۲٪، کدورت ۰/۹۷۹ و جذب مایع رویی ۰/۲۲۷ بودند. میکروکپسول‌ها با میکروسکوپ الکترونی روبشی، طیف‌سنجی فروسرخ تبدیل فوریه و کالری‌سنجی روبشی تفاضلی ارزیابی شدند. نتایج FTIR تشکیل کواسروات‌ها را تایید کرد. ترموگرام نقطه ذوب میکروکپسول بارگذاری شده $Q_{10}$ در نقطه ذوب آن (۵۰ درجه سلسیوس) به دلیل حلالیت آن در فاز روغن و به تله افتادن مناسب حین کپسولاسیون مشاهده نشد. رفتار رهایش $Q_{10}$ توسط مدل‌های مختلف ریاضی مورد بررسی قرار گرفت. ریزپوشینه‌های $Q_{10}$ برای غنی‌سازی شیر مورد استفاده قرار گرفت و نتایج نشان داد که میکروکپسول‌های پروتئین-کربوهیدرات توسعه یافته را می‌توان برای محافظت از ترکیبات آبگریز استفاده کرد.

**واژه‌های کلیدی:** انکپسولاسیون، ژلاتین، کوآنزیم $Q_{10}$، موسیلاژ دانه ریحان، ویژگی‌های فیزیکوشیمیایی

۱، ۲ و ۳- به‌ترتیب دانشجوی کارشناسی ارشد، استاد و دانشیار گروه علوم و صنایع غذایی، دانشکده کشاورزی، دانشگاه صنعتی اصفهان
(*- نویسنده مسؤل: Email: mfathi@iut.ac.ir)

DOI: 10.22067/ifstrj.2023.81438.1240